Multifunctionalized Gold Nanoparticles with Peptides Targeted to Gastrin-Releasing Peptide Receptor of a Tumor Cell Line

ARTICLE *in* BIOCONJUGATE CHEMISTRY · JUNE 2010

Impact Factor: 4.51 · DOI: 10.1021/bc1000164 · Source: PubMed

6 AUTHORS, INCLUDING:

Leticia Hosta-Rigau
Technical University of Denmark
34 PUBLICATIONS **960** CITATIONS
SEE PROFILE

Jordi Arbiol
Catalan Institute of Nanoscience and Nano…
347 PUBLICATIONS **7,635** CITATIONS
SEE PROFILE

Luis Javier Cruz
Leiden University Medical Centre
74 PUBLICATIONS **1,515** CITATIONS
SEE PROFILE

Marcelo J Kogan
University of Chile
70 PUBLICATIONS **1,780** CITATIONS
SEE PROFILE

Multifunctionalized Gold Nanoparticles with Peptides Targeted to Gastrin-Releasing Peptide Receptor of a Tumor Cell Line

Leticia Hosta-Rigau,[†] Ivonne Olmedo,[‡] Jordi Arbiol,[||] Luis J. Cruz,[†] Marcelo J. Kogan,*[,‡,§] and Fernando Albericio*[,†,⊥]

CIBER-BBN, Networking Centre on Bioengineering, Biomaterials and Nanomedicine, and Institute for Research in Biomedicine, Barcelona Science Park, Baldiri Reixac 10, 08028-barcelona, Spain, Division of Pharmacological and Toxicological Chemistry, School of Pharmacy and Chemistry, Casilla 233, University of Chile, Olivos 1007, Independencia, Santiago, Chile, Centre for Advanced Interdisciplinary Research in Material Sciences, Av. Blanco Encalada 2008, Santiago, Chile, Institucio Catalana de Recerca i Estudis Avançats (ICREA) and Institut de Ciencia de Materials de Barcelona, CSIC, Campus de la UAB, 08193 Bellaterra, CAT, Spain, and Department of Organic Chemistry, University of Barcelona, Martí i Franqués 1, 08028-barcelona, Spain. Received January 9, 2010; Revised Manuscript Received April 7, 2010

Functionalization of gold nanoparticles (AuNPs) with both a targeting peptide (an analogue of the peptide Bombesin) and a drug peptide ligand (an analogue of the RAF peptide) with the aim of improving selectivity in the delivery of the conjugates as well as the antitumor activity is described. Studies on the internalization mechanism of peptide−AuNP conjugates and viability of cells were carried out. An enhancement of the activity and selectivity of the peptide multifunctionalized conjugates was observed.

INTRODUCTION

Gold nanoparticles (AuNPs) have been extensively used in biological applications because of their biocompatibility, dimension, ease of characterization (*1, 2*), and rich history of surface chemistry. These features make these structures easily exploitable to meet the requirements of biomedical applications (*3*).

The size of AuNPs can be controlled from a few nanometers up to tens of nanometers, thereby placing them at dimensions that are smaller than or comparable to those of a cell (10−100 μm), a virus (20−450 nm), a protein (5−50 nm), or a gene (2 nm wide and 10−100 nm long). These sizes imply that they could get close to a biological target of interest (*4*). For example, AuNPs can be used to deliver a cargo, such as an anticancer drug, or a cohort of radionuclide atoms to a targeted region of the body, such as a tumor (*4*). On the other hand, AuNPs have been used in photothermal therapy for the destruction or molecular surgery of cancer cells or tumors. When irradiated with a focused laser in the near-infrared region (NIR) of suitable wavelength, targeted aggregates of AuNPs, nanorods, or nanoshells can kill bacteria (*5*) and cancer cells (*6*).

Thus, AuNPs provide an excellent intracellular targeting vector for two reasons: they can be synthesized routinely in appropriated sizes adequate for delivery varying from 0.8 to 200 nm with <10% size dispersity and can be modified with a large collection of small molecules, peptides, proteins, DNA, and polymers (*7*).

Surface modifications of AuNPs are often used to increase the functionality of nanoconjugates. These nanoparticle modifiers/conjugants include various peptides which can specifically recognize a target, thus improving cell type uptake (*8*) and ensuring that the AuNPs reach the desired target. Peptides attached to a single nanoparticle make the individual targeting signals more accessible to cell receptors (*9*), thus allowing them to participate in ligand−receptor interactions (*4, 10*).

The design and development of tumor-specific nanoparticles could significantly amplify the delivery capacity to a specific target of interest without affecting healthy cells. The target specificity of nanoparticles could be imparted by tagging with certain biovectors, which navigate them to particular organs or sites under in vivo conditions. The targeting vectors most commonly used are monoclonal antibodies and receptor-specific peptides. Monoclonal antibodies, due to their larger sizes, show poor in vivo mobility and thus delayed and reduced uptake over the desired target (*11–13*). Moreover, these antibodies are highly immunogenic and as such produce harmful side effects. In sharp contrast, peptides, which are smaller, offer various advantages, namely, rapid blood clearance, ease in the penetration of the tumor's vascular endothelium, increased diffusion rates in tissue, and low immunogenicity. Receptors for peptides are highly expressed on a variety of neoplastic and non-neoplastic cells. Furthermore, receptor-targeting peptides have shown a high level of internalization within tumor cells via receptor-mediated endocytosis. The capacity to internalize probes within tumor cells is crucial for delivering maximum payloads to tumor cells (*14–16*). These attractive physical properties coupled with their smaller size make peptides ideal candidates for developing new target-specific nanoparticles. In a recent paper, Chanda et al. conjugated a bombesin/gastrin-releasing peptide (BN/GRP) analogue to gold nanorods, which are internalized in cancer cells for the development of in vivo molecular imaging agents for cancer (*17*).

In the present study, we functionalized AuNPs with both a targeting peptide and a drug peptide ligand with the aim to improve not only the selectivity of the conjugates, but also their antitumor activity over the free drug. Since AuNPs conjugated to a targeting ligand have a higher capacity to enter cells, carrying the antitumor peptide and thus increasing its local concentration will, in turn, enhance the antitumor activity. BN was chosen as a targeting ligand for bombesin gastrin releasing

* To whom correspondence should be addressed. Phone: +34 934037088. Fax: +34 934037126. E-mail: albericio@pcb.ub.es, mkogan@ciq.uchile.cl.

[†] Barcelona Science Park.

[‡] University of Chile.

[§] Centre for Advanced Interdisciplinary Research in Material Sciences.

[||] ICREA and Institut de Ciencia de Materials de Barcelona.

[⊥] University of Barcelona.

10.1021/bc1000164
Published on Web 05/18/2010

Scheme 1. Multifunctionalization of Gold Nanoparticles with a Targeting Peptide (BN) and an Antitumoral Peptide (RAF)[a]

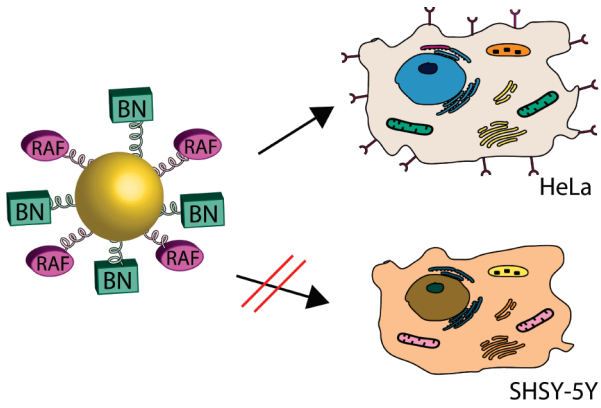

[a] BN recognizes the GRP receptor overexpressed in HeLA cells and not in the neuroblastoma line SHSY-5Y. The recognition mediates the penetration into HeLa cells.

peptide receptor (GRPr), which has been found to be overexpressed in prostate, breast, small cell lung, and cervical cancer (*14–20*). Furthermore, AuNPs were functionalized with the drug peptide ligand RAF analogue which inhibits Rb-Raf-1 binding in vivo and therefore inhibits tumor growth and angiogenesis (*21*). In addition, AuNPs were multifunctionalized with a mixture of both peptides with the goal of implementing the targeting vehicle with antitumor activity.

The size of AuNPs may affect the cell permeability as well as toxicity. Taking into account these relevant points in this study, we chose 20-nm-diameter gold nanoparticles for three reasons: (i) they possess a widespread organ distribution (*22–24*) which is very relevant for future drug delivery applications, (ii) they have higher penetration in cells with respect to bigger AuNP (>70 nm) (*25*), and last (iii) AuNPs of this size were reported to pose no inherent toxicity to different cell lines (*26, 27*) and in zebrafish embryos (*28*), in contrast to AuNPs of 1−2 nm that were found to be highly toxic in cell lines (*29, 30*).

The multifunctionalized AuNPs with RAF peptide analogues (Ac-Cys-Ahx-RAF) and BN (Ac-Cys-Ahx-BN) (Scheme 1) were evaluated for their cell internalization properties and in vitro viability in HeLa cells, which overexpress GPRr, and in neuroblastoma SHSH-5Y cells, which do not overexpress these receptors.

RESULTS AND DISCUSSION

BN and RAF Peptide Analogues. A very promising group of small targeting ligands comprises a number of regulatory peptides. Among these, the BN peptide, originally isolated from the skin of a frog, has also shown antitumor activity (*31*). BN-like peptides are known to bind to GRPrs with high affinity and specificity. A high number of GRPrs are overexpressed in various human tumors (*32*) like glioblastoma, small cell lung, gastric, pancreatic, prostate, breast, cervical, and colon cancer (*16, 33–36*), as well as in premalignant cells in the case of prostate, gastric, and lung cancers (*37–39*). These receptors are therefore promising targets for targeted therapy of cancer because of their location on the plasma membrane, which promotes the internalization of the receptor−ligand complex upon binding of a ligand. These findings open up the possibility of applying BN-like peptides as vehicles to deliver cytotoxic drugs (*40, 41*) into tumor cells (*42*). On the basis of studies by Dasgupta et al. (*21*), we selected the RAF peptide as the drug antitumor ligand. The retinoblastoma tumor suppressor protein (Rb) plays a vital role in regulating mammalian cell cycle progression and inactivation of this protein is required for entry into the S phase. Rb is inactivated by phosphorylation upon growth factor stimulation of quiescent cells, thereby facilitating the transition from G_1 to S phase (*43*). Previous studies have shown that the signaling kinase c-Raf (Raf-1) physically and functionally interacts with Rb and contributes to its inactivation, thereby facilitating cell proliferation. Disruption of the Rb-Raf-1 interaction by the 9-amino-acid peptide significantly inhibits Rb phosphorylation and thus cell proliferation (*21*).

Table 1. Structures of the Two Peptides Complexed to Gold Nanoparticles (Ac-Cys-Ahx-BN and Ac-Cys-Ahx-RAF) and the Two Fluorescently Labeled Peptides (Ac-Cys-Ahx-Lys(CF)-BN and Ac-Cys-Ahx-Lys(CF)-RAF) Used in This Study[a]

name	sequence
Ac-Cys-Ahx-BN	Ac*-Cys-Ahx**-Gln-Trp-Ala-Val-Gly-His-Leu-Met-NH_2
Ac-Cys-Ahx-RAF	Ac*-Cys-Ahx**-Gly-Ile-Ser-Asn-Gly-Phe-Gly-Phe-Lys-NH_2
Ac-Cys-Ahx-Lys (CF)-BN	Ac*-Cys-Ahx**-Lys(CF)-Gln-Trp-Ala-Val-Gly-His-Leu-Met-NH_2
Ac-Cys-Ahx-Lys (CF)-RAF	Ac*-Cys-Ahx**-Lys(CF)-Gly-Ile-Ser-Asn-Gly-Phe-Gly-Phe-Lys-NH_2

[a] * The N-terminus has been acetylated, ** aminohexanoic acid.

The peptides were synthesized using a Fmoc/^{t}Bu solid-phase synthetic strategy (Materials and Methods section) and a free thiol containing Cys was introduced at the end of a spacer to facilitate attachment onto the gold surface (Table 1). As the *C*-terminus of BN is required for high-affinity binding (*44*), the *N*-terminus of the peptide was modified through an aliphatic linker to allow labeling with the cargo (*45*). The spacers have to position the gold conjugate sufficiently far from the GRPr-binding region of BN to prevent hindrance of the binding (affinity) of the BN motif with GRPr (*46, 47*). The optimal hydrocarbon spacer length should vary from 3 to 8 carbon atoms without adversely affecting the resultant binding affinity (*48*). As reported by Hoffman et al. (*49*), an increase in the hydrophobicity of the linker group to excessive levels reduces the receptor-binding affinity (*47, 49, 50*).

Thus, for conjugating both BN and the RAF peptides, a 6-carbon-atom spacer (aminohexanoic acid, Ahx) was selected to be attached to a free thiol containing Cys in order to facilitate anchoring onto the gold surface (Ac-Cys-Ahx-BN and Ac-Cys-Ahx-RAF) (Table 1). To check whether the free analogue peptides—unconjugated to AuNPs—BN and RAF have the capacity to penetrate the cell, we labeled peptides with a carboxyfluorescein (CF) fluorophore. The CF was introduced into the ε-amino of an additional residue of Lys, which was incorporated at the *N*-terminal of the peptide, before the incorporation of the Ahx residue. Peptides Ac-Cys-Ahx-Lys(CF)-BN and Ac-Cys-Ahx-Lys(CF)-RAF were also produced using a Fmoc/^{t}Bu/Alloc solid-phase strategy (Supporting Information Figure S1, Table S1). The Alloc group was used to block the Lys side chain and was removed once the elongation of the peptide sequence was done to incorporate the CF before the global deprotection and cleavage.

Conjugation of Ac-Cys-Ahx-BN and Ac-Cys-Ahx-RAF with AuNPs. Ac-Cys-Ahx-BN and Ac-Cys-Ahx-RAF were conjugated separately and also in an equimolar mixture with a 20 nM AuNP solution to obtain the following conjugates: Ac-Cys-Ahx-BN@AuNPs, Ac-Cys-Ahx-RAF@AuNPs, and Ac-Cys-Ahx-BN/Ac-Cys-Ahx-RAF@AuNPs (Note: From a peptide point of view, a more correct nomenclature should be Ac-Cys(AuNPs)-Ahx-BN, Ac-Cys(AuNPs)-Ahx-RAF, and Ac-Cys(AuNPs)-Ahx-BN/Ac-Cys(AuNPs)-Ahx-RAF) (Table 1). We then tested the influence of both the targeting and drug ligands on the cell penetration and antitumor activity of these conjugates. AuNPs were obtained via the sodium citrate reduction method (*51–55*), which allows the synthesis of clusters of particles between 6 and 60 nm by adding various amounts of the reducing agent. The AuNPs were characterized by UV−vis (Figure 1) and transmission electron microscopy (TEM)

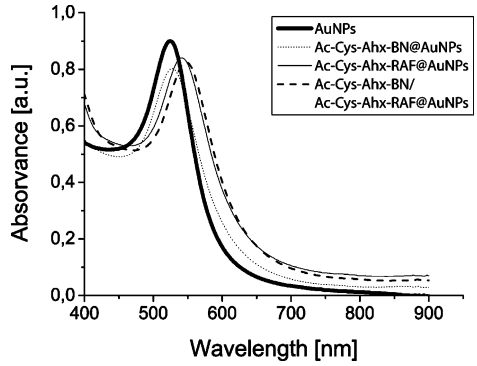

Figure 1. UV−vis spectra of AuNPs and their respective conjugates; a shift in the maximum is representative of the conjugation.

(Supporting Information Figure S3). The peptide-capped AuNPs were prepared by mixing a colloidal gold solution with an excess of peptide to obtain functionalized gold surfaces. The conjugates were characterized by using UV−vis spectroscopy, amino acid analysis (AAA), TEM, and electron energy loss spectroscopy (EELS).

Conjugation of Ac-Cys-Ahx-Lys(CF)-BN and Ac-Cys-Ahx-Lys(CF)-RAF with AuNPs. The same procedure described for the conjugation of Ac-Cys-Ahx-BN and Ac-Cys-Ahx-RAF to AuNPs was used to prepare Ac-Cys-Ahx-Lys(CF)-BN@AuNPs, Ac-Cys-Ahx-Lys(CF)-RAF@AuNPs, and Ac-Cys-Ahx-Lys(CF)-BN/Ac-Cys-Ahx-Lys(CF)-RAF@AuNPs.

Characterization of Conjugates. *UV−vis Spectroscopy.* The shift of the surface plasmon resonance band (SPR) to a longer wavelength (>522 nm with respect to the SPR of citrate AuNP, Figure 1), as a result of changes in the dielectric properties of the medium in which the AuNPs are found or the presence of materials adsorbed onto their surface, showed the capping of the AuNP surface with the peptide molecules (*4, 56*). The concentration of AuNPs was determined using the molar coefficient of extinction for the 20 nm AuNPs (5.41×10^8 M^{-1} cm^{-1}) as reported in the literature (*57*).

Electron Energy Loss Spectroscopy (EELS). To evaluate the presence of sulfur atoms and thus corroborate the functionalization of the AuNPs with the peptides, spectra between 140 and 220 eV were obtained on the AuNP surfaces for the conjugated and nonconjugated samples. An accurate analysis of the electron energy loss near the edge spectra (ELNES) at the S $L_{2,3}$ edge placed at around 165 eV was performed. All sample spectra show the S $L_{2,3}$ edge slope around 165 eV on the surface of the AuNPs, which is characteristic of peptide functionalization (Figure 2). Given that the nonconjugated sample was assumed to have a low number of S atoms, it was used to evaluate the signal-to-noise ratio in the S $L_{2,3}$ energy region. Table S2 (Supporting Information) shows a comparison of the maximum intensity obtained for the functionalized samples and the control. A slightly higher increment in intensity at 165 eV for the functionalized nanoparticles compared to the bare ones suggests that the thiol moiety of the peptides is attached to the AuNPs.

Determination of the Number of Peptide Molecules/Nanoparticle. To determine the number of peptide molecules per nanoparticle, the conjugates were centrifuged and the supernatants lyophilized, resuspended, and analyzed by HPLC to determine the amount of nonconjugated peptide by interpolation onto a calibration curve (Supporting Information Figure S2). Approximately 40% of the peptides used in the conjugation were attached to the AuNPs. In the case of the equimolar mixture of Ac-Cys-Ahx-BN and Ac-Cys-Ahx-RAF, 44% of the nonbounded peptide corresponds to Ac-Cys-Ahx-BN and 56% to Ac-Cys-Ahx-RAF. By subtracting the total amount of peptide used for the conjugation, the bounded peptide concentration was found to be about 50 μM and the AuNP solution was about 2 nM (determined spectrophotometrically), which results in a ratio of around 25 000 peptide molecules per AuNP. The large number of peptide molecules/nanoparticle could be attributed to a self-aggregation process that occurs in amphipathic peptides (*58*).

Amino Acid Analysis (AAA). The relationship among the concentrations of the amino acids His, Ile, and Phe give the relative concentration of these two peptides on the AuNPs. The relationship found, 1 for His/Ile and 2 for Phe/His, showed that both peptides were incorporated equimolarly onto the Ac-Cys-Ahx-BN/Ac-Cys-Ahx-RAF@AuNPs (Supporting Information Table S3).

Cellular Internalization of the Carboxyfluorescinated Peptides as Shown by Confocal Laser Scanning Microscopy (CLSM). Peptides Ac-Cys-Ahx-Lys(CF)-BN and Ac-Cys-Ahx-Lys(CF)-RAF were incubated with HeLa (cervical tumoral cell line which overexpresses GRP receptors) and SHSY-5Y cells for 24 h. As expected, Ac-Cys-Ahx-Lys(CF)-BN was efficiently internalized in HeLa cells and not in SHSY-5Y, while Ac-Cys-Ahx-Lys(CF)-RAF entered both HeLa and SHSY-5Y cell lines, hence showing its lack of specificity (Figure 3).

Accumulation of Peptide−AuNP Conjugates and AuNPs as Shown by CLSM. In order to prove whether the functionalization of AuNPs with BN and RAF—or with both together—favors selectivity in the delivery of the conjugates, the reflection of the nanoparticles was exploited. The red coloration of the nanoconjugates (*9*) of Ac-Cys-Ahx-BN and Ac-Cys-Ahx-RAF inside cells was observed due to the accumulation and reflection of the AuNP.

An internalization study of the conjugates after 24 h of incubation was performed in the tumoral cell line HeLa and in the SHSY-5Y cell line. The cell membrane was marked in green by WGA, and the nucleus was stained in blue with DRAQ5. The degree of accumulation inside the HeLa cells occurred in the following order Ac-Cys-Ahx-BN@AuNPs > Ac-Cys-Ahx-BN/Ac-Cys-Ahx-RAF@AuNPs > Ac-Cys-Ahx-RAF@AuNPs (Figure 4). Ac-Cys-Ahx-BN@AuNPs showed the greatest accumulation, suggesting a receptor-mediated internalization mechanism, most likely via endocytosis, as reported in the literature (*17*); however, in this paper we did not study the internalization mechanism. On the contrary, Ac-Cys-Ahx-RAF@AuNPs presented low internalization in HeLa cells due to the fact that the receptor-mediated internalization mechanism is not favored by target peptide. Finally, the conjugates Ac-Cys-Ahx-BN/Ac-Cys-Ahx-RAF@AuNPs showed an intermediate cell penetration capacity. As expected, gold conjugates did not accumulate in the SHSY-5Y cell line because of the low concentration of GRPr for this cell line.

These results provide an illustration of the power of our strategy. Thus, while the RAF conjugate internalizes poorly into HeLa cells, the AuNPs containing RAF and BN did because of the presence of the BN moiety, which has the capacity to bind to the GRPr of cells. Furthermore, the presence of the BN moiety provides selectivity for the drug−ligand conjugate as shown by the finding that none of the AuNPs penetrated the SHSY-5Y cells. This selectivity is potentially useful in the development of ligand-targeted therapeutics.

Colocalization of the Fluorescence and Gold Reflection Signal Caused by the Conjugate-Labeled Peptides as Shown by CLSM Imaging. The carboxyfluoresceinated conjugates, Ac-Cys-Ahx-Lys(CF)-BN@AuNPs, Ac-Cys-Ahx-Lys(CF)-RAF@AuNPs, and Ac-Cys-Ahx-Lys(CF)-BN/Ac-Cys-Ahx-Lys(CF)-RAF@AuNPs, were incubated with the tumor cell line HeLa for 24 h at 37 °C to colocalize the fluorescence signal caused by the peptide−AuNP conjugate and the reflection of the AuNP.

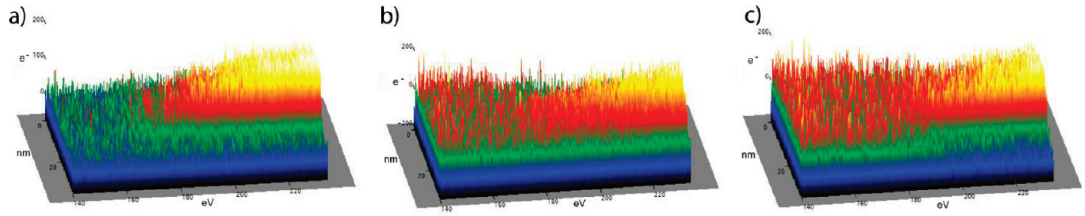

Figure 2. EELS spectrum obtained on the surface of (a) nonfunctionalized 20 nm AuNPs, (b) Ac-Cys-Ahx-BN functionalized AuNPs, and (c) Ac-Cys-Ahx-RAF functionalized AuNPs.

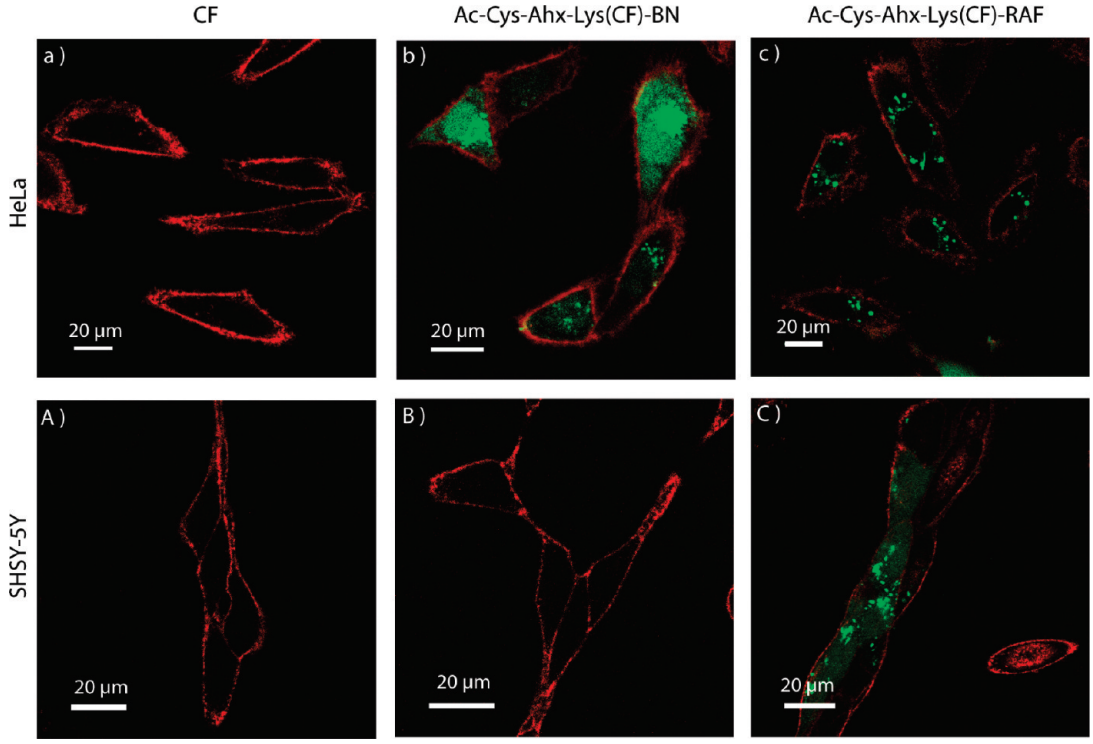

Figure 3. Localization of carboxyfluoresceinated peptides in HeLa cells (a−c) and in SHSY-5Y cells (A−D) incubated for 24 h. Control of CF (a, A), Ac-Cys-Ahx-Lys(CF)-BN (b, B), Ac-Cys-Ahx-Lys(CF)-RAF (c, C). Membranes (green) were stained with a fluorescence marker (WGA). The peptides were added at a final concentration of 1×10^{-5} M.

The membrane of the cells was stained green and the internalization of the fluorinated gold complexes was visualized using CLSM. These observations revealed that nearly all the AuNPs were complexed to the fluorescently labeled peptides (Figure 5) when overlapping the red reflection of the AuNPs with the blue fluorescence of the carboxyfluorinated peptides. These results indicate that the labeled peptides do not detach from the AuNP surface. However, a partial hydrolysis of the peptide in cells may occur. This possibility could not be discarded in the present study because the fluorescence label was found in the *N*-terminal extreme of the peptide, which was bound to the AuNPs surface.

Viability Studies. The degree of viability and effects of the free peptides (Ac-Cys-Ahx-BN and Ac-Cys-Ahx-RAF), gold conjugates Ac-Cys-Ahx-BN@AuNPs and Ac-Cys-Ahx-RAF@AuNPs, and the equimolar mixture Ac-Cys-Ahx-BN/Ac-Cys-Ahx-RAF@AuNPs and AuNPs on cell proliferation was determined by MTT assay in HeLa and SHSY-5Y cells following 24 h of incubation (Figure 6). AuNPs did not show any significant effects on HeLa cell viability, while Ac-Cys-Ahx-BN and Ac-Cys-Ahx-RAF at concentrations of 1×10^{-5} M reduced the viability of cells in 33% and 52%, respectively, with respect to the controls. As expected, the RAF peptide possesses a higher antitumor activity, since it is reported to suppress tumor growth and angiogenesis (*59, 60*). However, to the best of our knowledge, the antitumor activity of both peptides has never been compared in the same conditions. In the case of BN, the conjugation with AuNPs increases the toxicity in cells possibly due to a synergistic effect in the penetration between the AuNP and the peptide, which helps to increase the local concentration which in turn enhances the antitumor activity and is in accordance with the increased delivery of Ac-Cys-Ahx-BN-AuNP to HeLa cells. The conjugates Ac-Cys-Ahx-RAF-AuNP produce similar effects on cell viability with respect to the peptide Ac-Cys-Ahx-RAF-AuNP.

Interestingly, conjugates of the peptides with AuNPs did not show any effect on cell viability in neuroblastoma SHSY-5Y cells. The lack of toxicity could be attributed to the low penetration that the conjugates present in this cell line due to the low expression of GRPr receptors. Remarkably, Ac-Cys-Ahx-RAF is toxic against this cell line which evidences the low selectivity of this peptide against cells in general (as shown by the CLSM of the CF peptide, Figure 3); however, conjugation with AuNP results in increased selectivity (toxicity in HeLa cells but not in SHSY-5Y). The conjugation of this peptide with AuNPs could induce a change in the conformation of the peptide molecules that leads to a reduction of toxicity in neuroblastoma cells. This is an interesting point which we are currently studying.

CONCLUSIONS

In summary, we report herein a strategy to increase the activity and cell selectivity of AuNP−peptide conjugates by

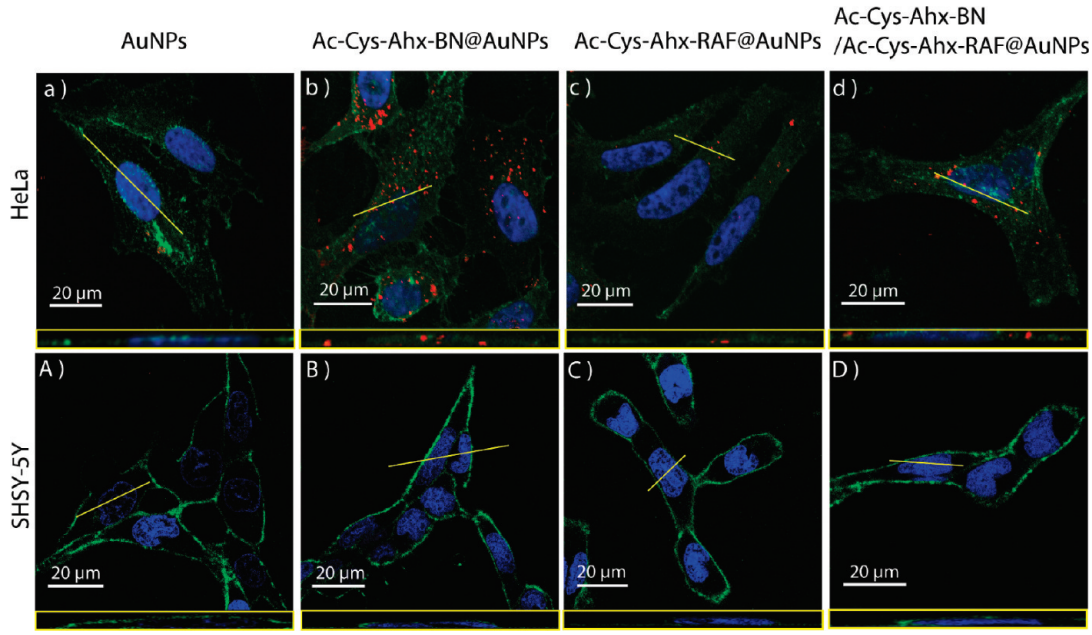

Figure 4. Localization of AuNPs and their conjugates in HeLa cells (a−d) and in SHSY-5Y cells (A−D) incubated for 24 h. AuNPs (a, A), Ac-Cys-Ahx-BN@AuNPs (b, B), Ac-Cys-Ahx-RAF@AuNPs (c, C), Ac-Cys-Ahx-BN/Ac-Cys-Ahx-RAF@AuNPs (d, D). The red dots represent reflections of groups of nanoparticles. Membranes (green) were stained with a fluorescence marker (WGA), and nuclei (blue) with a DNA marker (DRAQ5). The conjugated peptides were added at final concentrations of 1×10^{-5} M of peptides and 0.4 nM of AuNPs. The insets in yellow squares are the projection of the slides in the *z* axis to corroborate the localization of the gold nanoconjugates inside the cells and not onto the top of the cells.

means of the multifunctionalization of the AuNPs with a targeting peptide (BN) and an antitumor peptide (RAF). This work confirms that the conjugates in which BN is present penetrate cells that overexpress GRPr. However, a more detailed study of the internalization mechanism to confirm a receptor-mediated endocytosis mechanism in HeLa cells for the analogue of BN peptide is currently underway. The enhancement in activity and selectivity could contribute to a potential improvement of the efficacy of RAF for therapy by reducing the therapeutic index. Furthermore, this strategy will provide an opportunity for the controlled delivery of AuNPs used as cargoes for a localized (nanometrically) therapy like the so-called molecular surgery.

MATERIALS AND METHODS

Materials. Rink amide MBHA resin and Fmoc-N^{α}-protected amino acids were purchased from Iris Biotech GmbH (Marktredwitz, Germany). 7-Aza-1-hydroxy-1*H*-benzotriazole (HOAt) was obtained from GL Biochem (Shanghai, China); 1-benzotriazolyloxytris(pyrrolidino)-phosohonium hexafluorophosphate (PyBOP) was purchased from Novabiochem (Laüfelfelfingen, Switzerland); 7-azabenzotriazol-1-yloxytris(pyrrolidino)phosphonium hexafluorophosphate (PyAOP) from Applied Biosystems (Foster City, CA); *N,N*′-diisopropylethylamine (DIEA) from Albatros Chem. Inc. (Montreal, Canada); and *N,N*′-disopropylcarbodiimide (DIC) and triisopropylsilane (TIS) from Fluka Chemika (Buchs, Switzerland). 5(6)-Carboxyfluorescein (CF) was obtained from Acros (Somerville, NJ). Solvents for peptide synthesis and RP-HPLC were obtained from Scharlau (Barcelona, Spain). Trifluoroacetic (TFA) acid was supplied by KaliChemie (Bad Wimpfen, Germany). Dimethylformamide (DMF), dichoromethane (DCM), and acetonitrile (MeCN) were purchased from SDS (Peypin, France). Tetrakis(triphenylphosphine)palladium (0) [$Pd(PPh_3)_4$], phenyl silane ($PhSiH_3$), triisopropylsilane (TIS), and other chemicals used were obtained from Aldrich (Milwaukee, WI, USA) and were of the highest purity commercially available.

Peptide Synthesis and Chromatography. (All reported solvent ratios are expressed as v/v, unless otherwise stated). The four peptides were synthesized manually on Fmoc Rink amide MBHA resin (100 mg, 0.68 mmol/g) using a Fmoc/^{t}Bu strategy in polypropylene syringes, each fitted with a polyethylene porous disk. Solvents and soluble reagents were removed by suction. Washings between deprotection, couplings, and subsequent deprotection steps were carried out with DMF and DCM using around 10 mL solvent per gram of resin each time. The Fmoc group was removed by treatment with a mixture of piperidine−DMF (1:4 v/v) (2 × 10 min). After Fmoc removal, coupling reactions were carried out with Fmoc-amino acids (4 equiv), HOAt (4 equiv), and DIC (4 equiv) in DMF for 1.5 h. Couplings were monitored using the Kaiser test (*61*). When necessary, recouplings were done with PyBOP (4 equiv), HOAt (4 equiv), and DIEA (12 equiv) for 1.5 h. After completing the synthesis, we performed an acetylation step with a mixture of AcOH (10 equiv) and DIC (5 equiv) for 10 min. For fluorescently labeled peptides [Ac-Cys-Ahx-Lys(CF)-BN and Ac-Cys-Ahx-Lys(CF)-RAF], after completion of the peptide sequence, the Alloc (Allyloxycarbonyl) group was removed with $Pd(PPh_3)_4$ (0.1 equiv) in the presence of $PhSiH_3$ (10 equiv) (3 × 15 min) under Ar atmosphere followed by several washes (5 × 1 min) with sodium *N,N*′-diethyldithiocarbamate (0.02 M in DMF) and DMF. CF (5 equiv), PyAOP (5 equiv), HOAt (5 equiv), and DIEA (10 equiv) were dissolved in a mixture of DMF−DCM, preactivated for 10 min, and added to the peptidyl resin. The reaction mixture was stirred for 1.5 h. For the deprotection of side chain groups and concomitant cleavage of the peptides from the support, the resin was washed with DCM (3 × 1 min), dried, and treated with a TFA−H_2O−TIS (95:2.5:2.5) cocktail for 1 h. TFA was then removed by evaporation with a N_2 stream and peptides were precipitated with a mixture of cold anhydrous *tert*-butyl methyl ether (TBME) and hexane (2:1), dissolved in H_2O−MeCN (1:1) and freeze−dried. The crude peptides were purified using a semipreparative RP-HPLC [Waters 2487 Dual λ Absorbance Detector (Waters, MA, USA) equipped with a Waters 2700 Sample Manager, a Waters 600 controller, a Waters Fraction Collector, a Symmetry column (C_{18}, 5 μm, 30 × 100 mm), and Millenium software; flow rate = 10 mL/min, gradient = 0−20% B for 5 min, 20−40% B for 35 min, 40−100% B

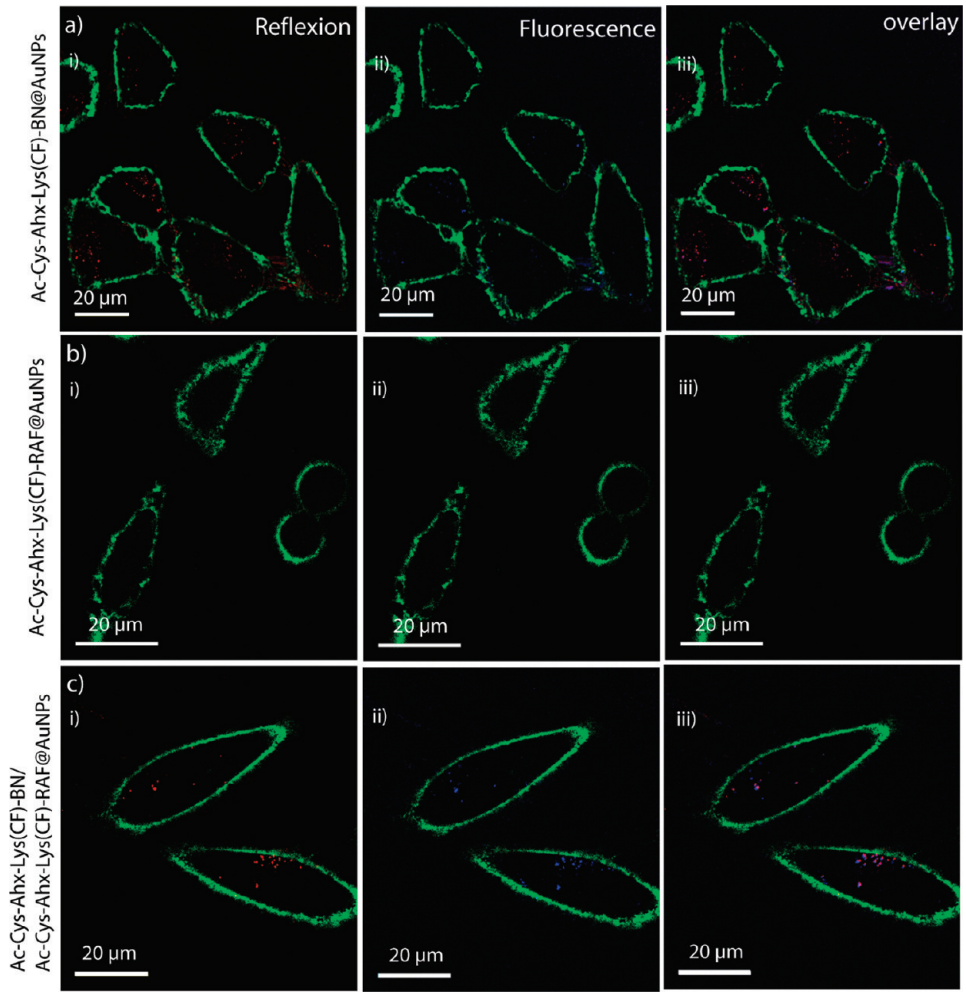

Figure 5. Localization of carboxyfluoresceinated peptides attached to AuNPs in HeLa cells incubated for 24 h. (a) Ac-Cys-Ahx-Lys(CF)-BN@AuNPs, (b) Ac-Cys-Ahx-Lys(CF)-RAF@AuNPs, (c) Ac-Cys-Ahx-Lys(CF)-BN/Ac-Cys-Ahx-Lys(CF)-RAF@AuNPs. Membranes (green) were stained with a fluorescence marker (WGA). Reflection of the AuNPs in red (i), carboxyfluorinated peptides in blue (ii), and the overlay of both channels in purple (iii). The conjugated peptides were added at a final concentration of 1×10^{-5} M of peptides and 0.4 nM of AuNPs.

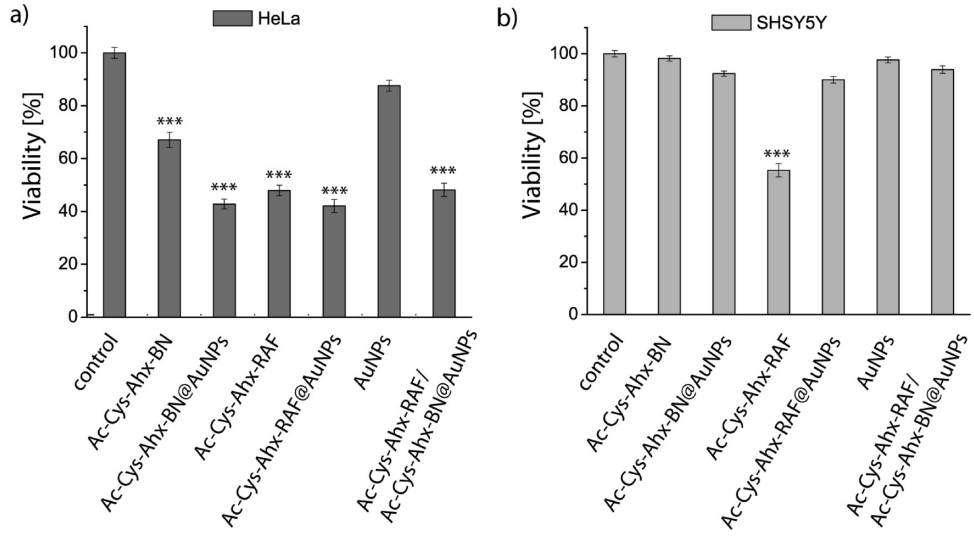

Figure 6. Cell viability assay after incubation of cells with Ac-Cys-Ahx-BN, Ac-Cys-Ahx-RAF, and their gold conjugates for 24 h: (a) HeLa cell line and (b) SHSY-5Y cell line. The conjugated and nonconjugated peptides were added at a final concentration of 1×10^{-5} M of peptides and 0.4 nM of AuNPs. The results are expressed as percentages compared to untreated cells and represent the mean ± standard deviation of three independent experiments (*** $P < 0.001$).

for 5 min (A = 0.1% TFA in H_2O, B = 0.05% TFA in MeCN)]. The purified peptides were identified (Supporting Information Figure S1 ai, bi, ci, di) at $\lambda = 220$ nm by analytical RP-HPLC [Waters 996 photodiode array detector equipped with Waters 2695 separation module, a Symmetry column (C_{18}, 5 μm, 4.6 × 150 mm) and Millennium software; flow rate = 1 mL/min, gradient = 20−40% D for 15 min for Ac-Cys-Ahx-BN, Ac-Cys-Ahx-RAF, Ac-Cys-Ahx-Lys(CF)-RAF, and 20−60% D for

15 min for Ac-Cys-Ahx-Lys(CF)-BN for 15 min (C = 0.045% TFA in H_2O, and D = 0.036% TFA in MeCN)]. Mass spectra were recorded on a MALDI Voyager DE RP time-of-flight (TOF) spectrometer (Applied Biosystems, Foster City, CA, USA) using ACH matrix (Supporting Information Figure S1 aii, bii, cii, dii).

Preparation of AuNPs. AuNPs were produced by reduction of $HAuCl_4 \times H_2O$ obtained from Aldrich (Milwaukee, WI, USA). $HAuCl_4 \times H_2O$ (8.7 mg) was added to a sodium citrate solution (100 mL, 2.2 mM) at reflux. The reducing agent was added rapidly, and the reaction was allowed to continue under uniform and vigorous stirring until a red wine color was observed (*58*).

Conjugation of Peptides with AuNPs. An excess of peptide was used for the conjugation (*62*). 1 mL of peptide solution (1 mg/mL in Milli-Q water) was added dropwise to 10 mL of AuNP solutions at room temperature with magnetic stirring, and the agitation was then maintained for 15 min. The conjugates were then purified by dialysis over three days in a Spectra/Por MWCO membrane: 6−8000 against 1 mM sodium citrate. The solution was refreshed six times to remove the excess peptide (Ac-Cys-Ahx-BN, Ac-Cys-Ahx-RAF, the equimolar mixture of Ac-Cys-Ahx-BN and Ac-Cys-Ahx-RAF or their fluorescently labeled counterparts).

UV−visible. UV−vis absorption spectra were recorded at room temperature with a 2501PC UV−vis recording spectrophotometer (Shimadzu Corporation, Kyoto, Japan).

Electron Energy Loss Spectroscopy (EELS). AuNP or AuNP-peptide (Ac-Cys-Ahx-BN@AuNPs, Ac-Cys-Ahx-RAF@AuNPs, Ac-Cys-Ahx-RAF/Ac-Cys-Ahx-BN@AuNPs) solutions (20 μL × 3) were placed on holley carbon Cu grids and allowed to dry at room temperature. Electron energy loss spectra were obtained in a Gatan Image Filter (GIF 2000) coupled to the JEOL 2010F microscope, with an energy resolution of 1.2 eV.

Amino Acid Analysis (AAA). Amino acid analysis was carried out by the AccQ. Tag method after acid hydrolysis with HCl (6N) for 24 h at 110 °C was used. The analysis was performed in a Waters Delta 600 RP-LC system with UV detection at 254 nm.

Determination of Conjugate Concentration. The number of peptides per particle was calculated by dividing the concentration of grafted peptide by the number of AuNPs in solution, which was determined spectrophotometrically considering the molar extinction coefficients detailed in the literature (*57*). The concentration of grafted peptide was determined by interpolation into a calibration curve (Supporting Information Figure S2) of the area of the HPLC peak of the solution resulting after centrifugation with an amicon filter (Amicon ultra-15, 3 kDa, MilliPore Corporation, Billerica, MA, USA) of a known volume of the conjugates at 13 500 rpm for 30 min. Once the AuNP pellet was removed, the free peptide containing solution was freeze−dried, dissolved again, and injected into the HPLC.

Cell Culture and Incubation with the Conjugates. HeLa and SHSY-5Y cell lines were obtained from ATCC no CCL-2 and ATCC no CRL-2266, respectively (Manasas, VA). Both cell lines were maintained in DMEM (low glucose medium for HeLa cell line and high glucose medium for SHSY-5Y) (Biological Industries) containing 10% fetal calf serum (FCS), 2 mM glutamine, 50 U/mL penicillin, and 0.05 g/mL streptomycin. For experiments, exponentially growing cells were detached from the culture flasks using a trypsin−0.25% ethylenediaminetetraacetic acid (EDTA) solution, and the cell suspensions were seeded at a concentration of 3.5×10^3 cells/cm^2 for the HeLa line and 1×10^3 cells/cm^2 for the SHSY-5Y line onto glass-bottom microwell dishes (35 mm Petri dish, 14 mm microwell, 1.5 mm cover glass) (Nalge Nunc International, Rochester, NY). Experiments were carried out 24 h later, when the confluence was approximately 70−80%. Nonadherent cells were washed away and attached cells were incubated at 37 °C in 5% CO_2 in DMEM with a known concentration of free AuNPs, peptide−AuNP conjugates, and carboxyfluorinated peptides. The conjugated and nonconjugated peptides were added in a 1:4 (conjugate/DMEM) ratio at a final concentration of 1×10^{-5} M of peptides and 0.4 nM of AuNPs.

MTT Assay. HeLa and SHSY-5Y viability in the presence of nonconjugated or conjugated nanoparticles and the free peptides was tested by the reduction of 3-[4,5-dimethylthiazol-2-yl]-2,5-diphenyltetrazolium bromide (MTT), including a control with no nanoparticles added. For each assay, 3.5×10^3 cells/cm^2 of the HeLa cell line and 1×10^3 cells/cm^2 of the SHSY-5Y cell line were seeded onto a 96-well plate (Nalge Nunc) and cultured for 24 h. The conjugates were added in a 1:4 (conjugate/DMEM) ratio, and the free peptides were added at the same concentration as the peptide−gold conjugates at a final concentration of 1×10^{-5} M of peptides and 0.4 nM of AuNPs. Cells were incubated for 22 h at 37 °C under a 5% CO_2 atmosphere. After incubation, the medium was removed and the cells were incubated with 200 μL fresh medium containing MTT (0.5 mg/mL) for 2 h. The resulting blue formazan was solubilized in 150 μL acidified isopropanol (0.04 M HCl) and the absorbance was measured at 560 nm using a plate reader (Multiskan Ascent, Thermo Scientific). The values of the untreated cells were taken as 100%, and cell viability was expressed as a percentage of the untreated cells. The data were obtained from three independent experiments performed in triplicate.

Confocal Laser Scanning Microscopy (CLSM). For the cellular localization of AuNP conjugates (Ac-Cys-Ahx-BN@AuNPS, Ac-Cys-Ahx-RAF@AuNPs, Ac-Cys-Ahx-BN/Ac-Cys-Ahx-RAF@AuNPs) and for the carboxyfluorinated peptides (Ac-Cys-Ahx-Lys(CF)-BN and Ac-Cys-Ahx-Lys(CF)-RAF), HeLa and SHSY-5Y cells were plated onto glass coverslips, grown to 60% confluence, and then incubated at 37 °C under a 5% CO_2 atmosphere with either Ac-Cys-Ahx-Lys(CF)-BN, Ac-Cys-Ahx-Lys(CF)-RAF or nanoparticle conjugates for 24 h. WGA as plasma membrane marker and DRAQ5 as a DNA dye were added just before recording the image. The samples were examined using an Olympus Fluoview 500 confocal microscope with a 60×/1.4 NA objective.

ACKNOWLEDGMENT

We gratefully acknowledge Tommaso Cupido for their helpful discussions. We thank Raquel Garcia Olivas, and Elisenda Coll (UB-SCT) for their assistance with CLSM and TEM, respectively. This work was partially supported by AECID, FONDECYT 1090143 CICYT (CTQ2009-07758), the Instituto de Salud Carlos III (CB06_01_0074), the Generalitat de Catalunya (2009SGR 1024), the Institute for Research in Biomedicine, and the Barcelona Science Park.

Supporting Information Available: Additional information as described in the text. This material is available free of charge via the Internet at http://pubs.acs.org.

LITERATURE CITED

(1) Sokolov, K., Follen, M., Aaron, J., Pavlova, I., Malpica, A., Lotan, R., and Richards-Kortum, R. (2003) Real-time vital optical imaging of precancer using anti-epidermal growth factor receptor antibodies conjugated to gold nanoparticles. *Cancer Res. 63*, 1999–2004.

(2) Elghanian, R., Storhoff, J. J., Mucic, R. C., Letsinger, R. L., and Mirkin, C. A. (1997) Selective colorimetric detection of polynucleotides based on the distance-dependent optical properties of gold nanoparticles. *Science 277*, 1078–1081.

(3) Bhattacharya, R., Mukherjee, P., Xiong, Z., Atala, A., Soker, S., and Mukhopadhyay, D. (2004) Gold nanoparticles inhibit VEGF165-induced proliferation of HUVEC cells. *Nano Lett. 4*, 2479–2481.

(4) Kogan, M. J., Olmedo, I., Hosta, L., Guerrero, A. R., Cruz, L. J., and Albericio, F. (2007) Peptides and metallic nanoparticles for biomedical applications. *Nanomedicine 2*, 287–306.

(5) Zharov, V. P., Mercer, K. E., Galitovskaya, E. N., and Smeltzer, M. S. (2006) Photothermal nanotherapeutics and nanodiagnostics for selective killing of bacteria targeted with gold nanoparticles. *Biophys. J. 90*, 619–627.

(6) Zharov, V. P., Galitovskaya, E. N., Johnson, C., and Kelly, T. (2005) Synergistic enhancement of selective nanophotothermolysis with gold nanoclusters: Potential for cancer therapy. *Lasers Surg. Med. 37*, 219–226.

(7) Tkachenko, A. G., Xie, H., Liu, Y. L., Coleman, D., Ryan, J., Glomm, W. R., Shipton, M. K., Franzen, S., and Feldheim, D. L. (2004) Cellular trajectories of peptide-modified gold particle complexes: Comparison of nuclear localization signals and peptide transduction domains. *Bioconjugate Chem. 15*, 482–490.

(8) Thurn, K. T., Brown, E. M. B., Wu, A., Vogt, S., Lai, B., Maser, J., Paunesku, T., and Woloschak, G. E. (2007) Nanoparticles for applications in cellular Imaging. *Nanoscale Res. Lett. 2*, 430–441.

(9) Tkachenko, A. G., Xie, H., Coleman, D., Glomm, W., Ryan, J., Anderson, M. F., Franzen, S., and Feldheim, D. L. (2003) Multifunctional gold nanoparticle-peptide complexes for nuclear targeting. *J. Am. Chem. Soc. 125*, 4700–4701.

(10) Efremov, R. G., Chugunov, A. O., Pyrkov, T. V., Priestle, J. P., Arseniev, A. S., and Jacoby, E. (2007) Molecular lipophilicity in protein modeling and drug design. *Curr. Med. Chem. 14*, 393–415.

(11) Pissuwan, D., Valenzuela, S. M., Miller, C. M., and Cortie, M. B. (2007) A golden bullet? Selective targeting of toxoplasma gondii tachyzoites using anti body-functionalized gold nanorods. *Nano Lett. 7*, 3808–3812.

(12) Souza, G. R., Christianson, D. R., Staquicini, F. I., Ozawa, M. G., Snyder, E. Y., Sidman, R. L., Miller, J. H., Arap, W., and Pasqualini, R. (2006) Networks of gold nanoparticles and bacteriophage as biological sensors and cell-targeting agents. *Proc. Natl. Acad. Sci. U.S.A. 103*, 1215–1220.

(13) Qian, X. M., Peng, X. H., Ansari, D. O., Yin-Goen, Q., Chen, G. Z., Shin, D. M., Yang, L., Young, A. N., Wang, M. D., and Nie, S. M. (2008) In vivo tumor targeting and spectroscopic detection with surface-enhanced Raman nanoparticle tags. *Nat. Biotechnol. 26*, 83–90.

(14) Scopinaro, F., De Vincentis, G., and Varvarigou, A. D. (2005) Use of radiolabeled bombesin in humans. *J. Clin. Oncol. 23*, 3170–3171.

(15) Bartholdi, M. F., Wu, J. M., Pu, H. F., Troncoso, P., Eden, P. A., and Feldman, R. I. (1998) In situ hybridization for gastrin-releasing peptide receptor (GRP receptor) expression in prostatic carcinoma. *Int. J. Cancer 79*, 82–90.

(16) Markwalder, R., and Reubi, J. C. (1999) Gastrin-releasing peptide receptors in the human prostate: Relation to neoplastic transformation. *Cancer Res. 59*, 1152–1159.

(17) Chanda, N., Shukla, R., Katti, K. V., and Kannan, R. (2009) Gastrin releasing protein receptor specific gold nanorods: breast and prostate tumor avid nanovectors for molecular imaging. *Nano Lett. 9*, 1798–1805.

(18) Schwartsmann, G., DiLeone, L. P., Horowitz, M., Schunemann, D., Cancella, A., Pereira, A. S., Richter, M., Souza, F., da Rocha, A. B., Souza, F. H., Pohlmann, P., and de Nucci, G. (2006) A phase I trial of the bombesin/gastrin-releasing peptide (BN/GRP) antagonist RC3095 in patients with advanced solid malignancies. *Invest. New Drugs 24*, 403–412.

(19) Varvarigou, A., Bouziotis, P., Zikos, C., Scopinaro, F., and De Vincentis, G. (2004) *Cancer Biother. Radiopharm. 19*, 219–229.

(20) Cornelio, D. B., Meurer, L., Roesler, R., and Schwartsmann, G. (2007) Gastrin-releasing peptide receptor expression in cervical cancer. *Oncology 73*, 340–345.

(21) Dasgupta, P., Sun, J. Z., Wang, S., Fusaro, G., Betts, V., Padmanabhan, J., Sebti, S. M., and Chellappan, S. P. (2004) Disruption of the Rb-Raf-1 interaction inhibits tumor growth and angiogenesis. *Mol. Cell. Biol. 24*, 9527–9541.

(22) Kim, J. H., Kim, K.-W., Kim, M. H., and Yu, Y. S. (2009) Intravenously administered gold nanoparticles pass through the blood-retinal barrier depending on the particle size, and induce no retinal toxicity. *Nanotechnology 20*, 505101–9.

(23) De Jong, W. H., Hagens, W. I., Krystek, P., Burger, M. C., Sips, A. J., and Geertsma, R. E. (2008) Particle size-dependent organ distribution of gold nanoparticles after intravenous administration. *Biomaterials 29* 1912–9.

(24) Sonavane, G., Tomoda, K., and Makino, K. (2008) Biodistribution of colloidal gold nanoparticles after intravenous administration: effect of particle size. *Colloids Surf., B 66*, 274–80.

(25) Chithrani, D. B., Ghazani, A. A., and Chan, W. C. W. (2006) Determining the size and shape dependence of gold nanoparticle uptake into mammalian cells. *Nano Lett. 6* (4), 662–668.

(26) Connor, E. E., Mwamuka, J., Gole, A., Murphy, C., and Wyatt, M. D. (2005) Gold nanoparticles are taken up by human cells but do not cause acute cytotoxicity. *Small 1* (3), 325–327.

(27) Kahn, J., Oillai, B., Das, T. K., Singh, Y., and Maiti, S. (2007) Molecular effects of uptake of gold nanoparticles in HeLa cell. *ChemBiochem 8*, 1237–1240.

(28) Bar-Ilan, O., Albrecht, R. M., Fako, V. E., and Furgeson, F. (2009) Toxicity assessments of multisized gold and silver nanoparticles in zebrafish embryos. *Small 5* (16), 1897–1910.

(29) H-Pan, Y., Neuss, S., Leifert, A., Fischler, M., Wen, F., and Simon, U. (2007) Size-dependent cytotoxicity of gold nanoparticles. *Small 3* (11), 1941–1949.

(30) Tsoli, M., Kuhn, H., Brandau, W., Esche, H., and Schmid, G. (2005) Cellular uptake and toxicity of Au55 clusters. *Small 1* (8−9), 841–844.

(31) Nagy, A., Armatis, P., Cai, R. Z., Szepeshazi, K., Halmos, G., and Schally, A. V. (1997) Design, synthesis, and in vitro evaluation of cytotoxic analogs of bombesin-like peptides containing doxorubicin or its intensely potent derivative, 2-pyrrolinodoxorubicin. *Proc. Natl. Acad. Sci. U.S.A. 94*, 652–656.

(32) Reubi, J. C. (1995) Neuropeptide receptors in health and disease - the molecular-basis for in-vivo imaging. *J. Nucl. Med. 36*, 1825–1835.

(33) Moody, T. W., Mahmoud, S., Staley, J., Naldini, L., Cirillo, D., South, V., Felder, S., and Kris, R. (1989) Human glioblastoma cell-lines have neuropeptide receptors for bombesin gastrin-releasing peptide. *J. Mol. Neurosci. 1*, 235–242.

(34) Moody, T. W., Carney, D. N., Cuttitta, F., Quattrocchi, K., and Minna, J. D. (1985) High-affinity receptors for bombesin GRP-like peptides on human small cell lung-cancer. *Life Sci. 37*, 105–113.

(35) Qin, Y. F., Ertl, T., Cai, R. Z., Halmos, G., and Schally, A. V. (1994) Inhibitory effect of bombesin receptor antagonistic RC-3095 on the growth of human pancreatic-cancer cells in-vivo and in-vitro. *Cancer Res. 54*, 1035–1041.

(36) Yano, T., Pinski, J., Groot, K., and Schally, A. V. (1992) Stimulation by bombesin and inhibition by bombesin gastrin-releasing peptide antagonist RC-3095 of growth of human breast-cancer cell-lines. *Cancer Res. 52*, 4545–4547.

(37) Preston, S. R., Woodhouse, L. F., Jonesblackett, S., Miller, G. V., and Primrose, J. N. (1995) High-affinity binding-sites for gastrin-releasing peptide on human colorectal-cancer tissue but not uninvolved mucosa. *Br. J. Cancer 71*, 1087–1089.

(38) Shriver, S. P., Bourdeau, H. A., Gubish, C. T., Tirpak, D. L., Davis, A. L. G., Luketich, J. D., and Siegfried, J. M. (2000) Sex-specific expression of gastrin-releasing peptide receptor: Relationship to smoking history and risk of lung cancer. *J. Natl. Cancer Inst. 92*, 24–33.

(39) Lin, K. S., Luu, A., Baidoo, K. E., Hashemzadeh-Gargari, H., Chen, M. K., Pili, R., Pomper, M., Carducci, M., and Wagner, H. N. (2004) A new high affinity technetium analogue of bombesin containing DTPA as a pharmacokinetic modifier. *Bioconjugate Chem. 15*, 1416–1423.

(40) Schally, A. V., and Nagy, A. (1999) Cancer chemotherapy based on targeting of cytotoxic peptide conjugates to their receptors on tumors. *Eur. J. End. 141*, 1–14.

(41) Szereday, Z., Schally, A. V., Nagy, A., Plonowski, A., Bajo, A. M., Halmos, G., Szepeshazi, K., and Groot, K. (2002) Effective treatment of experimental U-87MG human glioblastoma in nude mice with a targeted cytotoxic bombesin analogue, AN-215. *Br. J. Cancer 86*, 1322–1327.

(42) Zhang, H. W., Chen, J. H., Waldherr, C., Hinni, K., Waser, B., Reubi, J. C., and Maecke, H. R. (2004) Synthesis and evaluation of bombesin derivatives on the basis of pan-bombesin peptides labeled with indium-111, lutetium-177, and yttrium-90 for targeting bombesin receptor-expressing tumors. *Cancer Res. 64*, 6707–6715.

(43) Wang, S., Ghosh, R. N., and Chellappan, S. P. (1998) Raf-1 physically interacts with Rb and regulates its function: a link between mitogenic signaling and cell cycle regulation. *Mol. Cel. Biol. 18*, 7487–7498.

(44) Moody, T. W., Crawley, J. N., and Jensen, R. T. (1982) Pharmacology and neurochemistry of bombesin-like peptides. *Peptides 3*, 559–563.

(45) Hoehne, A., Mu, L., Honer, M., Schubiger, P. A., Ametamey, S. M., Graham, K., Stellfeld, T., Borkowski, S., Berndorff, D., Klar, U., Voigtmann, U., Cyr, J. E., Friebe, M., Dinkelborg, L., and Srinivasan, A. (2008) Synthesis, F-18-labeling, and in vitro and in vivo studies of bombesin peptides modified with silicon-based building blocks. *Bioconjugate Chem. 19*, 1871–1879.

(46) Hoffman, T. J., Quinn, T. P., and Volkert, W. A. (2001) Radiometallated receptor avid peptide conjugates for specific targeting of cancer cells. *J. Nucl. Med. 28*, 527–539.

(47) Hoffman, T. J., Gali, H., Smith, C. J., Sieckman, G. L., Hayes, D. L., Owen, N. K., and Volkert, W. A. (2003) Novel series of In-111-labeled bombesin analogs as potential radiopharmaceuticals for specific targeting of gastrin-releasing peptide receptors expressed on human prostate cancer cells. *J. Nucl. Med. 44*, 823–831.

(48) Abd-Elgaliel, W. R., Gallazzi, F., Garrison, J. C., Rold, T. L., Sieckman, G. L., Figueroa, S. D., Hoffman, T. J., and Lever, S. Z. (2008) Design, synthesis, and biological evaluation of an antagonist-bombesin analogue as targeting vector. *Bioconjugate Chem. 19*, 2040–2048.

(49) Hoffman, T. J., Simpson, S. D., Smith, C. J., Simmons, J., Siekman, G. L., Higginbotham, C., Eshima, D., Volkert, W., and Thornback, J. R. (1999) Accumulation and retention of Tc-99m RP591 by GRP receptor expressing tumours in SCID mice. *Eur. J. Nucl. Med. 26*, PS416.

(50) Hoffman, T. J., Smith, C. J., Simpson, S. D., Sieckman, G. L., Higginbotham, C., Jimenez, H., Eshima, D., Thornback, J. R., and Volkert, W. A. (2000) Optimizing pharmacokinetics of Tc-99m-GRP receptor targeting peptides using multi-amino acid linking groups. *J. Nucl. Med. 41*, 1013.

(51) Bauer, G., Hassmann, J., Walter, H., Haglmuller, J., Mayer, C., and Schalkhammer, T. (2003) Resonant nanocluster technology - from optical coding and high quality security features to biochips. *Nanotechnology 14*, 1289–1311.

(52) Hogemann, D., Ntziachristos, V., Josephson, L., and Weissleder, R. (2002) High throughput magnetic resonance imaging for evaluating targeted nanoparticle probes. *Bioconjugate Chem. 13*, 116–121.

(53) Liu, J. Q., Zhang, Q., Remsen, E. E., and Wooley, K. L. (2001) Nanostructured materials designed for cell binding and transduction. *Biomacromolecules 2*, 362–368.

(54) Marinakos, S. M., Anderson, M. F., Ryan, J. A., Martin, L. D., and Feldheim, D. L. (2001) Encapsulation, permeability, and cellular uptake characteristics of hollow nanometer-sized conductive polymer capsules. *J. Phys. Chem. B 105*, 8872–8876.

(55) West, J. L., and Halas, N. J. (2000) Applications of nanotechnology to biotechnology - Commentary. *Curr. Opin. Biotechnol. 11*, 215–217.

(56) McLean, J. A., Stumpo, K. A., and Russell, D. H. (2005) Size-selected (2−10 nm) gold nanoparticles for matrix assisted laser desorption ionization of peptides. *J. Am. Chem. Soc. 127*, 5304–5305.

(57) Haiss, W., Thanh, N. T. K., Aveyard, J., and Fernig, D. G. (2007) Determination of size and concentration of gold nanoparticles from UV-Vis spectra. *Anal. Chem. 79*, 4215–4221.

(58) Hosta, L., Pla-Roca, M., Arbiol, J., Lopez-Iglesias, C., Samitier, J., Cruz, L. J., Kogan, M. J., and Albericio, F. (2009) Conjugation of Kahalalide F with gold nanoparticles to enhance in vitro antitumoral activity. *Bioconjugate Chem. 20*, 138–146.

(59) Davis, R. K., and Chellappan, S. (2008) Disrupting the Rb-Raf−1 interaction: a potential therapeutic target for cancer. *Drug News Persp. 21*, 331–335.

(60) Ciuffreda, L., McCubrey, J. A., and Milella, M. (2009) Signaling intermediates (PI3K/PTEN/AKT/mTOR and RAF /MEK/ERK pathways) as therapeutic targets for anti-cancer and anti- angiogenesis treatments. *Curr. Signal Transduction Ther. 4*, 130–143.

(61) Kaiser, E., Colescott, R L., Bossinger, C. D., and Cook, P. I. (1970) Color test for detection of free terminal amino groups in the solid-phase synthesis of peptides. *Anal. Biochem. 34*, 595–598.

(62) Olmedo, I., Araya, E., Sanz, F., Medina, E., Arbiol, J., Toledo, P., Alvarez-Lueje, A., Giralt, E., and Kogan, M. J. (2008) How changes in the sequence of the peptide CLPFFD-NH2 can modify the conjugation and stability of gold nanoparticles and their affinity for β-amyloid fibrils. *Bioconjugate Chem. 19*, 1154–63.

BC1000164